Optical Modeling of Nanocrystalline TiO_2 Films

Akira Usami*,† and Hajime Ozaki‡

Central Research Institute of Electric Power Industry, 2-11-1 Iwatokita, Komae-shi, Tokyo 201-8511, Japan, and Department of Electrical Engineering and Bioscience, Waseda University, 3-4-1 Okubo, Shinjuku-ku, Tokyo 169-8555, Japan

Received: February 27, 2004; In Final Form: October 7, 2004

The light transmittance, T, in nanocrystalline TiO_2 films was studied as a function of the light wavelength, λ, the nanocrystal radius, a, and the film thickness, d. Two types of TiO_2 nanoparticles were employed: a commercial powder (P25) and synthesized particles from titanium isopropoxide (SP). The X-ray diffraction measurements revealed that both P25 and SP are mainly anatase and the average crystal sizes, $2a$, of P25 and SP are 50.3 and 23.7 nm, respectively. Despite the visual difference between micron-order thin films of P25 and SP, the light hemispherical transmittance corrected with the surface specular reflectance has a clear dependence of $\ln(T) = -0.5\beta\lambda^{-4}a^3d$, with $\beta = 1.5 \times 10^3$ from visible to near-infrared wavelengths. The dependence and β value were successfully explained by the simplest model on the basis of the Rayleigh scattering theory. This indicates that the nanocrystalline TiO_2 thin films are a typical medium where the simplest scattering model is a good approximation. However, the model was inapplicable to light scattering in relatively thick P25 films of 1.5−3.0 μm because of nonnegligible internal multiple scattering. For the moderate thickness films, $\ln(T) \propto \lambda^{\gamma}$, where γ increases from -4 in proportion to the film thickness is an alternative approximation. With these light scattering models, the light absorption rate of the TiO_2 crystal was successfully evaluated from experimental extinction rates.

1. Introduction

Recently, there has been increasing interest in the unique functions of nanocrystalline and microcrystalline semiconductors.[1] Solar cells,[2−5] electrochromic displays,[6] and photocatalytical self-cleaning films[7] exemplify some novel optical applications of nanocrystalline and microcrystalline semiconductor films. In these optically functioning inhomogeneous films, quantitative evaluation of optical properties is very important for both devise design and fundamental material characterization. Light propagation in inhomogeneous media depends on absorption and scattering; the extinction rate is the sum of the absorption and scattering rates.[8−10] If the light scattering is negligible, inhomogeneous media are assumed to be apparently uniform media, having effective refractive indices; effective medium theories such as the Bruggeman model have been employed. However, since many of the important semiconductor nanoparticles have nonnegligible light scattering because of large refractive indices, light scattering is generally essential for optical evaluation in nanocrystalline and microcrystalline films. In fact, in microcrystalline Si films, significant modification of optical responses by light scattering has been reported.[11,12] Additionally, a nonnegligible influence of light scattering on an electrical response has also been reported in nanocrystalline TiO_2 films.[13] Thus, a quantitatively valid model for the internal light scattering of nanocrystalline and microcrystalline semiconductor films is significant.

Unfortunately, the light scattering in inhomogeneous media is generally a very complex phenomenon because of rescattering and the interaction of scattered light (multiple scattering and dependent scattering, respectively).[14] Thus, quantitative theoretical evaluation of the light scattering is usually very difficult. Several groups have attempted the evaluation of the light scattering properties for, for exmaple, nanocrystalline Si and TiO_2.[11,12,15−19] Although some results qualitatively explained the experimental results, a quantitatively valid theoretical evaluation has not been presented except for that employing empirical values in crucial parameters.

In this paper, we discuss light scattering in nanocrystalline TiO_2 films. An advantage of the utilization of nanocrystalline TiO_2 films is that TiO_2 is a very stable material having a high refractive index. Another advantage is the optical properties of nanocrystalline TiO_2 films themselves are very important, owing to the recent novel photoelectrochemical applications. Here, the light transmittance in nanocrystalline TiO_2 films was experimentally studied as a function of the light wavelength, the nanocrystal radius, and the film thickness. As a result, a clear dependence of the transmittance on these parameters was found in thin films; the dependence is successfully explained by the simplest model for light scattering from a dense medium. A light scattering model for moderate thickness films is also discussed.

2. Theoretical Framework

The theme of this paper is the modeling of light scattering in extremely dense media. Unfortunately, discussion based on the first-principle theory is difficult for light scattering in dense media. Additionally, a theoretical discussion only for the specialists is not the aim of this paper; this paper attempts to present a simple approximation that satisfactorily characterizes experimental results. At this stage, the approximation is unknown; however, since we will demonstrate in the Results and Discussion section that light scattering in nanocrystalline

* Corresponding author. E-mail: usami@criepi.denken.or.jp.
† Central Research Institute of Electric Power Industry.
‡ Waseda University.

10.1021/jp040178y CCC: $30.25
Published on Web 01/15/2005

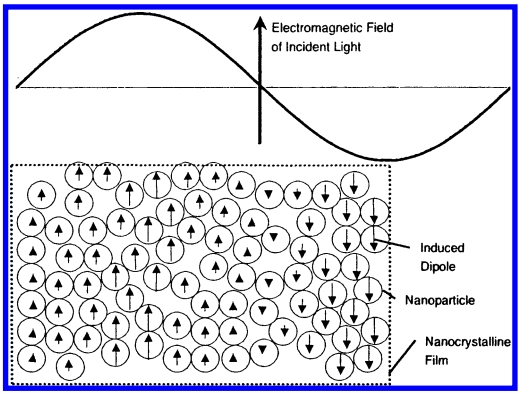

Figure 1. Schematic image of the light scattering mechanism of nanocrystalline films. The incident light has an electromagnetic field (upper curve). In each particle, a dipole field (arrow) is induced, owing to dielectric polarization. Since the intensity of the dipole fields (arrow length) depends on the local intensity of the electromagnetic field of the light, the dipole intensity fluctuates temporally, owing to the light propagation. The temporal fluctuation induces a new electromagnetic wave radiation; this radiation is observed as scattered light. The total scattered light is the sum of the radiations from all the particles. It should be noted that the particles in the image are enlarged for the explanation; the real nanoparticles are much smaller than the wavelengths of visible light. Details of the explanation are presented in the text.

TiO_2 thin films depends on the simplest model for light scattering from a dense medium, the simplest scattering model is summarized in this section in advance.

Physically, light scattering by dielectric particles is explained as follows (a schematic image is shown in Figure 1). In a dielectric particle embedded in an electric field, electric charges due to dielectric polarization are induced. Since light is an electromagnetic wave, light has a spatially and temporally fluctuating electromagnetic field. Thus, the induced charges fluctuate temporally. Since this fluctuation of the charges induces a new electromagnetic wave radiation, the induced radiation is observed as light scattering. If the particle is much smaller than the incident light wavelength, the induced charges are approximately a dipole because the electromagnetic field of the incident light is assumed to be spatially uniform over the particle. This scattering is referred to as the Rayleigh scattering. Therefore, the simplest light scattering model for films consisting of randomly distributing small particles is described as the sum of the radiation fields from the randomly distributing dipoles induced in each particle. The scattering rate, α, for the simplest model has already been presented:[10]

$$\alpha = \beta\lambda^{-4}a^3 \tag{1}$$

where λ is the wavelength of incident light and a is the radius of a particle. In eq 1, β depends on the refractive index, fractional volume, and distribution of the particles;[10] when the total scattering field is the sum of independent dipole fields (i.e., the optical interactions between the dipole fields are negligible), β is formulated analytically with the refractive indices of the particles, n_s, and the nanocrystalline film, n,[20] and the fractional particle volume, f,[8−10]

$$\beta = 2f(2\pi n)^4\left|\frac{n_s^2 - n^2}{n_s^2 + 2n^2}\right|^2 \tag{2}$$

The light hemispherical (collimated + diffuse) transmittance, T, is related to α as $T = (1 - R)\exp(-\alpha d/2)$, where R is the specular reflectance on the film surface and d is the film thickness. Here, since forward scattering, which has the same intensity as backward scattering owing to symmetry in the Rayleigh scattering, is detected as diffuse transmission, an effective scattering rate is assumed to be $\alpha/2$. Consequently, the following dependence of T on λ, a, and d is provided.

$$\ln(T) \propto \frac{\beta(f, n_s, n)}{2}\lambda^{-4}a^3 d \tag{3}$$

A detailed discussion is also presented in the Appendix.

Finally, we mention a caveat. In the model, internal multiple scattering between the scattering centers is neglected. However, for intensified scattering in thick films, the multiple scattering is not negligible. The multiple scattering effects are discussed in the last subsection of the Results and Discussion section.

3. Experimental Section

The preparation of the nanocrystalline TiO_2 films basically followed preparation methods for dye-sensitized solar cells.[3,4,22] Thus, the resultant films are essentially the same as those in the solar cells except for nonsensitization and somewhat thin thickness. The nanocrystalline TiO_2 films were prepared by spreading slurries of TiO_2 particles on substrates. Two slurries were prepared: one slurry was prepared from a commercial TiO_2 powder (P25, Nippon Aerosil), which is a prevailing one in the applications,[3] and another was prepared from particles (SP) synthesized from titanium isopropoxide with the method of ref 4, which is also a prevailing method for the solar cells. Since the dry powder P25 consists of clusters of the primary nanoparticles, these clusters should be broken into the separate nanoparticles by force. We employed ultrasonic agitation (Sharp, UT-53N, 35 kHz, 55 W) for the separation. Acetylacetone and poly(ethylene glycol) (PEG, average molecular weight 20 000) were added as stabilizers for the P25 dispersion. The slurry composition is 3.0 g of P25, 12 mL of water, 0.24 mL of acetylacetone, 1.2 g of PEG, and a drop of Triton X-100. The preparation of thicker films in subsection 4.4 was carried out by increasing the P25 concentration (at most, 1.7-fold as dense as above). The slurry of SG was prepared with the method in ref 4. All the slurries were spread on substrates by spin-coating. Bare glass and F-doped SnO_2-coated glass (FTO, Asahi Glass) were employed as the substrates. The quality of the nanocrystalline films depended strongly on the wetting of the substrates; a selection of the substrates was due to the wetting. The spin-coated films were dried for more than 20 min under the ambient air. Subsequently, the films were fired for 30 min at 450 °C in the ambient air; this annealing decomposes the additives and leaves porous TiO_2 alone on the substrates. The resultant films were visually clear/transparent for SP and translucent but lustrous without any cracks for P25.

The light hemispherical transmittance of the nanocrystalline films on the substrates was measured with a Shimazu MPC3100 instrument. In the measurements, the samples were illuminated from the nanocrystalline film sides; the transmitted light, which is the sum of the collimated and forward scattering light, was detected with an integrating sphere. In subsection 4.4, R is required. We have the Shimazu MPC3100 experimental unit for the evaluation of R, although the incident light angle, θ, normal to the surface is not 0° but 12°. Experimental results with the unit revealed little dependence of R on λ from near-infrared wavelengths to short wavelengths where light absorption by TiO_2 is nonnegligible. Thus, we conclude that R depends on surface morphology rather than bulk properties. On the basis of the wavelength independence of R, we estimate R from a

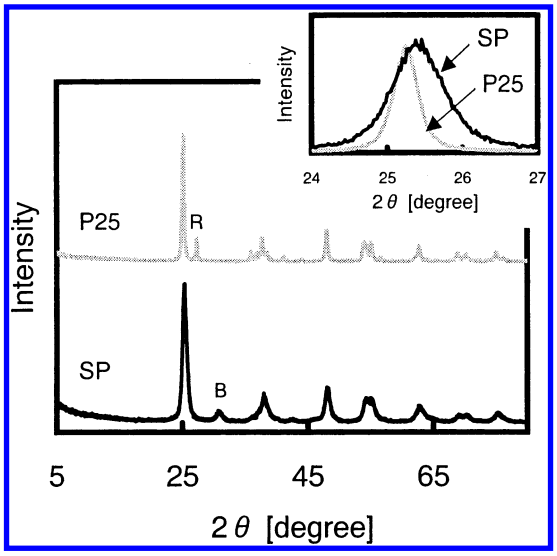

Figure 2. Powder XRD spectra of P25 and SP. SP represents particles synthesized from titanium isopropoxide with the method of ref 4. R and B stand for peaks of rutile and brookite, respectively. All the other peaks are of anatase. The inset shows the peaks around 25.4°.

long wavelength. The film thickness was estimated from an optical interference property in the films;[23,24] in order to check this estimation, measurements with a surface profiler were also carried out. Particle characterization of the crystal size and structure was conducted with powder X-ray diffraction (XRD) measurements; the crystal size was estimated with the Scherrer equation.[25]

4. Results and Discussion

4.1. Material Characterization. Equation 3 indicates the light transmittance depends on the refractive index and size of the nanocrystals. TiO_2 has the three crystal structures: anatase, rutile, and brookite; the refractive indices are not all the same. The crystal size has a more significant influence; that is, the scattering rate is the third order in crystal size. Thus, the particle characterization is very important. For the characterization, powder XRD measurements were carried out. The results are shown in Figure 2. The peak angles indicate that both P25 and SP are mainly anatase, though some small peaks of rutile and brookite are also detected in P25 and SP, respectively. Thus, these have approximately the same refractive index as that of anatase. The inset is an enlargement of the peaks at 25.4°. The crystal size depends on the full width at half-maximum of the diffraction peaks; the estimated crystal diameters of SP and P25 are 23.7 and 50.3 nm on average, respectively.

4.2. Light Transmittance in Thin Films of P25. We studied the light hemispherical transmittance, T, in the nanocrystalline TiO_2 films as a function of the light wavelength, λ, the nanocrystal radius, a, and the film thickness, d. That is, the dependence of T on λ was investigated by varying a and d. First, we fix both a and d in this subsection. The experimental results in nanocrystalline thin films of P25 are shown in Figure 3a. These films were visually translucent; in agreement with the look, relatively large light scattering losses are detected.

The oscillation appreciable at long wavelengths is ascribed to optical interference in the films. The peak (or dip) wavelengths depend on d.[23,24] Thus, the film thicknesses were estimated from the oscillation. For the lower curve in Figure 3a, since both the nanocrystalline and FTO films cause the interference, the oscillation structures of the two films mix. Thus, to estimate the nanocrystalline film thickness, we must decompose the mixing structure. The decomposition was carried out by referring to T of the FTO substrate depicted in the inset of Figure 3a. The estimations indicated that both the films are $d \approx 1$ μm.

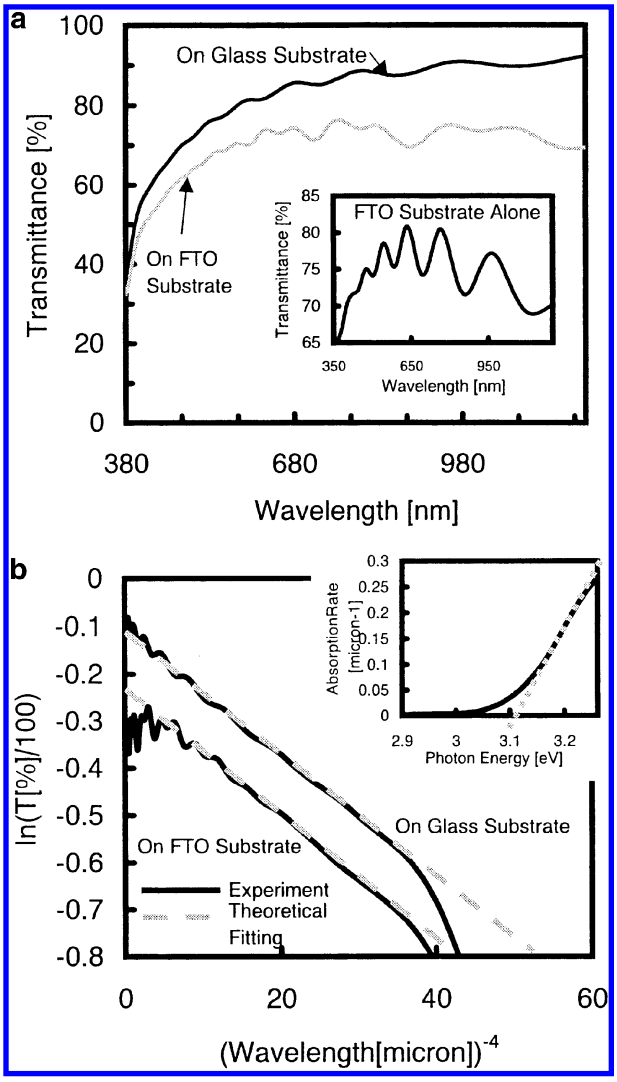

Figure 3. Light transmittances of P25 nanocrystalline thin films and the FTO substrate. T versus λ (a) and the replotting of ln(T) versus λ^{-4} (b) are depicted. The solid curves are experimental; the difference of the curves is due to the substrates of the films. Both the films are ~1 μm thick. The inset of part a shows transmittance data of the FTO substrate alone. The dashed lines in part b are the theoretical fittings of the experimental results with eq 3. The inset of part b shows the light absorption rate evaluated from the experimental extinction rate and the theoretical fitting of the scattering rate. The dashed line in the inset of part b is a guide to compare the absorption rate with that in Figure 6.

Equation 3 of the simple scattering model suggests that the dependence of T on λ should be $\ln(T) \propto \lambda^{-4}$. The replotting of ln($T$) versus λ^{-4} is depicted as the solid curves in Figure 3b. The dashed lines in Figure 3b are theoretical fittings of the experimental results with the dependence of $\ln(T) \propto \lambda^{-4}$. The theoretical fittings agree well with the experimental results, except for small and large λ^{-4}.

The deviation of the experimental results from the theoretical fittings at the large λ^{-4} is ascribed to light absorption by the TiO_2 crystals. This is because the experimental results, which are the extinction rates, are affected by both light absorption and light scattering, while the theoretical fittings represent the light scattering rates alone. In other words, the light absorption rate is evaluated from the deviation at the large λ^{-4}. The

absorption rate estimated from the deviation is depicted in the inset of Figure 3b. The onset of the absorption is 3.0 eV; the absorption increases significantly until around 3.2 eV and, then, increases moderately. From the XRD measurements, P25 is a compound of anatase and rutile. The absorption onset agrees with the band gap energy of rutile; 3.2 eV is the band gap energy of anatase. The significant increase of the light absorption is explained by exponentially tailing band gap states that stem from the rutile constituent in the anatase-based compound. Thus, the estimation of the absorption rate agrees with the material characterization. The following should be noted: if the light scattering was negligible, the extinction rate would be equated with the absorption rate; however, because of the significant light scattering, the quantitative evaluation of the scattering rate is indispensable for the accurate evaluation of the absorption rate of the nanocrystalline films.

The discrepancy at small λ^{-4} is appreciable only in the lower curve. This discrepancy is probably attributed to an influence of the FTO substrate, that is, low transmittances of the FTO substrate at long wavelengths. In fact, the T value of the nanocrystalline film with the FTO substrate is limited by the T value of the FTO substrate at long wavelengths, as shown in Figure 3a.

Finally, from the theoretical fittings (the dashed lines), an experimental value of β is estimated, $\beta = 1.5 \times 10^3$. Estimating n_s, n, and f, the theoretical value of β can be calculated with eq 2. The XRD measurements indicate that the main crystal structure of the particles is anatase; thus, n_s is assumed to be the refractive index of anatase, 2.5. From the literature, n and f are approximately 1.6[27] and 0.5,[28] respectively. The resultant theoretical value of β is 1.1×10^3 (more detailed theoretical evaluations of β indicate $\beta = (1.0 \pm 0.2) \times 10^3$, as shown in the Appendix). The calculated β value is close to the experimental result. This suggests that the simple theory is a good approximation for the light scattering in the nanocrystalline TiO_2 thin films. However, the discrepancy between these β values is not a numerical error because of the uncertainty of the parameters. The discrepancy is probably attributed to a multiple scattering effect. This will be discussed in subsection 4.4.

4.3. Dependence of Light Transmittance on Crystal Size and Film Thickness. Equation 3 indicates T depends not only on λ but also on a and d. The latter dependence was studied, using the nanocrystalline films prepared from SP on the FTO substrates. The results are shown in Figure 4; the $2a$ and d values of each film are shown in the figure. The upper two solid curves in Figure 4 are the experimental results of the nanocrystalline films prepared from SP. These films were visually transparent; in contrast to the look, nonnegligible light scattering is shown in the figure. The lowest solid curve in Figure 4 is the same as the lower curve of Figure 3b; the dashed line is the theoretical fitting. As discussed above, the XRD measurements reveal that the refractive indices of P25 and SP are assumed to be that of anatase. Thus, β is expected to be independent of the particle type; that is, the value of β estimated from the dashed line is applicable to SP as well. The dotted−dashed line and the dot−dot−dashed line are the calculation results with eq 3: $\beta = 1.5 \times 10^3$, $2a = 23.7$ nm, and $d = 5.0$ μm for the dotted−dashed line and $\beta = 1.5 \times 10^3$, $2a = 23.7$ nm, and $d = 2.5$ μm for the dot−dot−dashed line. The comparisons between the experimental results and the theoretical calculations indicate satisfactory agreement between them except for large λ^{-4}. The deviation at $\lambda^{-4} > \sim 40$ μm^{-4} is due to the light absorption by the TiO_2 nanocrystals. The nanocrystalline films prepared from P25 were visually quite different from those of SP: the nanocrystalline films of P25 were translucent, while the nanocrystalline films of SP were transparent. The agreement between the experimental results and the theoretical predictions clearly indicates that the light scattering of all the visually different films is explained by the simple theoretical model.

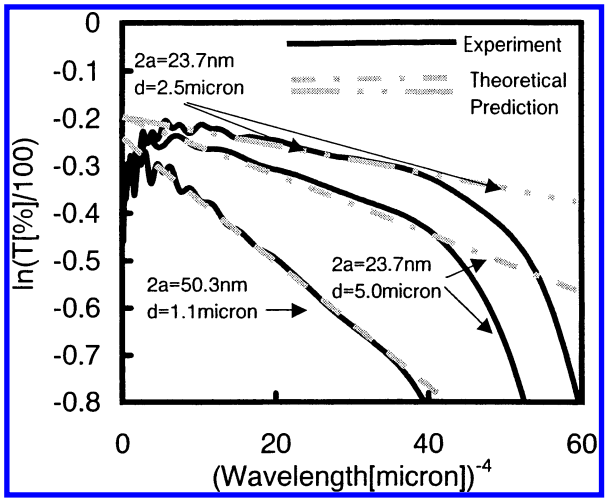

Figure 4. Dependence of transmittance spectra on the crystal size and the film thickness. The solid curves are experimental. The upper two curves are the results of the films prepared from SP; the lowest curve is that of the film of P25, which is the same as the lower curve in Figure 3b. All the films were prepared on the FTO substrates. The experimental crystal size, $2a$, and film thickness, d, are included in the figure. The dotted−dashed and dot−dot−dashed lines are the theoretical calculation results with the parameter values and eq 3. β employed in the theoretical predictions was estimated from the dashed line, which is the theoretical fitting in Figure 3b.

4.4. Light Transmittance of Moderate Thickness Films. We have shown the simplest light scattering model is a good approximation for the evaluation of the light scattering rates in the nanocrystalline TiO_2 thin films. In the thin films, a single ray of light traversing the volume is expected to be scattered only once before leaving the medium. However, in thicker nanocrystalline films, more than one scattering is expected to occur per ray; that is, nonnegligible influences of the internal multiple scattering, which is neglected in the simplest model, are expected. Thus, it is important to show how the multiple scattering changes the model. Unfortunately, as mentioned above, theoretical discussion of the multiple scattering in the dense media is very difficult. Thus, we attempt the experimental characterization of multiple scattering effects in moderate thickness films. First, since a remarkable feature of the light scattering in the thin films is the wavelength dependence of the transmittance, $\ln(T) \propto \lambda^{-4}$, we assume $\ln(T) \propto \lambda^{\gamma}$ in moderate thickness films. Figure 5 shows film thickness variations in $\ln[-\ln(T/(1 - R))]$ versus $\ln(\lambda)$, where the slope is γ. The oscillation of the curves is the optical interference in the films. Neglecting the oscillation, all the experimental results in Figure 5 fit to straight lines. This indicates each film has a definite value of γ; thus, the assumption of $\ln(T) \propto \lambda^{\gamma}$ is valid in the wavelengths.

In the inset of Figure 5, the dependence of γ on the film thickness is shown. The inset shows γ has a linearly increasing profile from -4 at a 0 μm thickness with increasing film thickness. Since γ for the single scattering is -4, it is reasonable that the extrapolated value of γ to a 0 μm thickness is -4. This also supports the validity of the assumption of $\ln(T) \propto \lambda^{\gamma}$. Additionally, however, this indicates that, in principle, the single scattering occurs only at a 0 μm thickness; that is, rigorously, the multiple scattering occurs even in very thin films. Thus, as

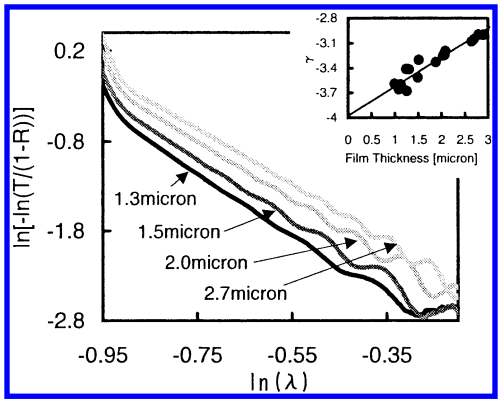

Figure 5. Light transmittance spectra of moderate thickness films prepared of P25. Assuming $\ln(T) \propto \lambda^{\gamma}$, the slope of $\ln[-\ln(T/(1-R))]$ versus $\ln(\lambda)$ is γ. R stands for the surface specular reflectance. In the inset, the estimated γ is depicted as a function of the film thickness.

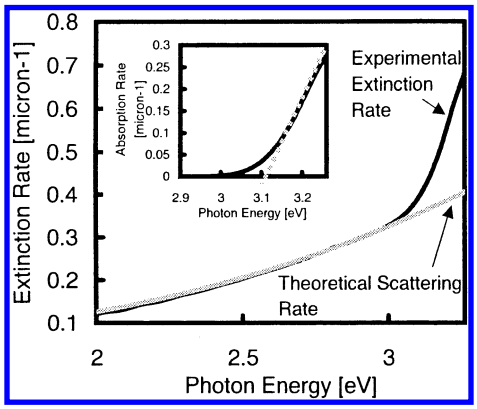

Figure 6. Extinction, scattering, and absorption rates of a P25 moderate thickness film. The black curve and the shadow curve are an experimental extinction rate and the theoretical fitting of the scattering rate with $\gamma = -3$, respectively. The film consists of P25; the film thickness is 2.7 μm. The evaluated absorption rate is shown in the inset. The dashed line in the inset is a guide to compare the absorption rate with that in Figure 3b.

mentioned above, the independent scattering model is not the exact model but an approximation even for the thin films. As γ increases linearly, we cannot define a thicker limit of the approximation. However, from subsection 4.2, around 1 μm is reasonable as a practical limit in the P25 films, that is, a scattering reflectance smaller than ~35%. For thicker films, $\ln(T) \propto \lambda^{\gamma}$, where γ has a linear dependence on the film thickness, is an alternative. For example, $\gamma \geq -3$, rather than $\gamma = -4$, is appropriate for the P25 films thicker than 2.5 μm. Figure 6 shows the theoretical fitting with $\gamma = -3$ for the P25 film of a 2.7 μm thickness. This indicates that the theoretical fitting with $\gamma = -3$ is a good approximation of the scattering rate. We can further check the validity from the evaluation of the absorption rate. The absorption rate evaluated from the experimental extinction rate and the theoretical scattering rate is depicted in the inset of Figure 6. The absorption rate in Figure 6 should be the same as the inset of Figure 3b because both of the films consist of P25. The results clearly indicate that the inset of Figure 6 is the same as the inset of Figure 3b. The light scattering in Figure 6 has a wavelength dependence different from that of Figure 3; thus, this agreement strongly supports the validity of the alternative model.

5. Conclusions

This paper has presented clear evidence that nanocrystalline TiO_2 thin films are a typical inhomogeneous medium explained by the simplest model for light scattering from a dense medium. That is, the total scattering field is the sum of the radiation fields from all the dipoles induced in each randomly distributing nanoparticle by the electromagnetic field of incident light. This scattering model predicts the clear dependence of T on λ, a, and d: $\ln(T) \propto 0.5\beta\lambda^{-4}a^3d$; the light transmittance experiments with the material characterization by powder XRD measurements have demonstrated the theoretical prediction. For the moderate thickness films, the internal multiple scattering effects were pronounced. In this case, the dependence of $\ln(T) \propto \lambda^{\gamma}$ is a good approximation, taking $\gamma > -4$. With these light scattering models, the light absorption rate of the TiO_2 crystals was successfully evaluated from the experimental extinction rates.

Acknowledgment. The authors thank Takashi Tamura of Waseda University for the AFM measurements, Daisuke Sugiyama of Central Research Institute of Electric Power Industry (CRIEPI) for the XRD measurements, and Dr. Sadao Higuchi of CRIEPI for the surface profiler measurements.

Appendix

In the text, only the results of theoretical evaluations of β are presented. We have also conducted detailed theoretical evaluations of β: $\beta = (1.0 \pm 0.2) \times 10^3$.

The accurate evaluation of β requires discussion of the following: (1) refractive index of P25, n_s, (2) wavelength dependence of n_s, (3) volume fraction of TiO_2, f, (4) refractive index of the nanocrystalline film, n, and (5) modeling itself. Each is discussed in detail as follows.

(1) Refractive index of P25, n_s.

P25 is not a single crystal of anatase. The volume fraction of rutile, f_R, is calculated from the peak intensity of rutile, I_R, and anatase, I_A.[30] In our XRD measurements,

$$I_R/I_A = 0.170 \tag{1A}$$

$$\text{weight \% of anatase: } W_A\,(\text{wt \%}) = \frac{100.0}{1.000 + 1.265\dfrac{I_R}{I_A}} = 82.3\ (\text{wt \%}) \tag{2A}$$

Considering the specific gravity difference of rutile and anatase, f_R (vol %) = 16.6 (vol %).

Employing the following equation for an average refractive index,[9] n_s is

$$n_s = n_A\left[1 + \frac{3f_R\left(\dfrac{n_R - n_A}{n_R + 2n_A}\right)}{1 - f_R\left(\dfrac{n_R - n_A}{n_R + 2n_A}\right)}\right] = 2.56 \tag{3A}$$

(we assume refractive indices of anatase of $n_A = 2.52$ and rutile of $n_R = 2.76$ here).

(2) Wavelength dependence of n_s.

The wavelength dependence of n_s is evaluated with the above method for each wavelength. The results are shown in Table 1.

(3) Volume fraction of TiO_2, f.

The pores in the nanocrystalline films were created by annealing decomposition of poly(ethylene glycol) (PEG). Thus,

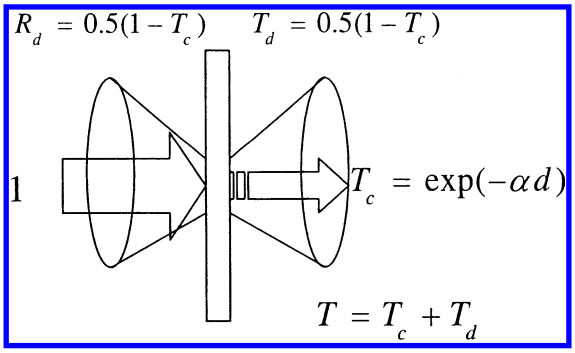

Figure 7. Scheme of light scattering.

TABLE 1: Summary of the Evaluation of β ($x = \exp(-\alpha d/2)$)

wavelength (nm)	refractive index			β ($\times 10^3$) ($T = 0.5(1 + x^2)$; $f = 0.43$, $n = 1.6$)	β ($\times 10^3$) ($T = x$; $f = 0.43$, $n = 1.6$)
	anatase	rutile	P25		
436	2.77	2.85	2.78	1.4	1.1
492	2.66	2.72	2.67	1.2	1.1
546	2.60	2.65	2.61	1.1	1.0
578	2.57	2.62	2.58	1.1	1.0
691	2.51	2.56	2.52	1.0	1.0
706	2.51	2.55	2.52	1.0	1.0

the most simple and reliable equation for f is

$$f = \frac{W_{TiO_2}/\rho_{TiO_2}}{W_{TiO_2}/\rho_{TiO_2} + W_{PEG}/\rho_{PEG}} \quad (4A)$$

where W is the weight of the slurry and ρ is the specific gravity. Here, each value is the following: $W_{TiO_2} = 3.0$ g, $W_{PEG} = 1.2$ g, $\rho_{TiO_2} = 4.0$ g cm^{-3}, $\rho_{PEG} = 1.2$ g cm^{-3}. The resultant f value is 0.43. We consider this to be a reasonable value.

(4) Refractive index of the nanocrystalline film, n.

The evaluation of n is described in ref 27. The error in n is $< \pm 10\%$. The resultant error in β is less than that in n because the terms of the fourth-power parentheses and the second-power brackets in eq 2 cancel. The resultant error in β is at most 7%.

(5) Modeling.

In Figure 7, a schematic image of light scattering is shown, where T_c is collimated transmittance, T_d is diffused transmittance, and R_d is diffused reflectance. Here, an incident light intensity of 1 and no light absorption are assumed. Using the symmetry in the Rayleigh scattering, the total transmittance, T, is obtained as $T = T_c + T_d = 0.5[1 + \exp(-\alpha d)]$. In the model of the text, we assumed $T = \exp(-\alpha d/2)$. The assumption is valid when the light scattering is small, such as thin films where the single Rayleigh scattering is a good approximation.

However, at short wavelengths in the P25 films, the light scattering seems to not be small. A reason the model of the text ($T = \exp(-\alpha d/2)$) is a good approximation even at short wavelengths is that this model compensates for the wavelength dependence of the refractive index. A quantitative result is shown in Table 1. As shown in Table 1, the text model can explain the light scattering at the whole of the wavelengths with a small error in β.

Considering these things, the resultant β value is $(1.0 \pm 0.2) \times 10^3$ (± 0.1 is from Table 1 and ± 0.1 is from (4); ± 0.2 is the sum).

Note Added after ASAP Publication. This article was published ASAP on January 15, 2005 with an error in eq 3A. The correct version was reposted on January 19, 2005.

References and Notes

(1) Trindade, T.; O'Brien, P.; Pickett, N. L. *Chem. Mater.* **2001**, *13*, 3843.
(2) O'Regan, B.; Grätzel, M. *Nature (London)* **1991**, *353*, 737.
(3) Nazeeruddin, M. K.; Kay, A.; Rodicio, I.; Humphry-Baker, R.; Müller, E.; Liska, P.; Vlachopoulos, N.; Grätzel, M. *J. Am. Chem. Soc.* **1993**, *115*, 6382.
(4) Barbe, C. J.; Arendse, F.; Comte, P.; Jirousek, M.; Lenzmann, F.; Shklover, V.; Grätzel, M. *J. Am. Ceram. Soc.* **1997**, *80*, 3157.
(5) Vetterl, O.; Finger, F.; Carius, R.; Hapke, P.; Houben, L.; Kluth, O.; Lambertz, A.; Mück, A.; Rech, B.; Wagner, H. *Sol. Energy Mater. Sol. Cells* **2000**, *62*, 97.
(6) Bechinger, C.; Ferrere, S.; Zaban, A.; Sprague, J.; Gregg, B. A. *Nature (London)* **1996**, *383*, 608.
(7) Heller, A. *Acc. Chem. Res.* **1995**, *28*, 503.
(8) Ishimaru, A. *Wave Propagation and Scattering in Random Media*; Academic Press: New York, 1978.
(9) Bohren, C. F.; Huffman, D. R. *Absorption and Scattering of Light by Small Particles*; Wiley: New York, 1983.
(10) Tsang, L.; Kong, J. A.; Shin, R. T. *Theory of Microwave Remote Sensing*; Wiley: New York, 1985.
(11) Ferrand, P.; Romestain, R. *Appl. Phys. Lett.* **2000**, *77*, 3535.
(12) Jun, K. H.; Carius, R.; Stiebig, H. *Phys. Rev. B* **2002**, *66*, 115301.
(13) Tachibana, Y.; Hara, K.; Sayama, K.; Arakawa, H. *Chem. Mater.* **2002**, *14*, 2527.
(14) Tien, C. L.; Drolen, B. L. *Annu. Rev. Numer. Fluid Mech. Heat Transfer* **1987**, *1*, 1.
(15) Ferber, J.; Luther, J. *Sol. Energy Mater. Sol. Cells* **1998**, *54*, 265.
(16) Ferber, J.; Baumgärtner, S.; Luther, J. *Proceedings of the 2nd World Conference and Exhibition on Photovoltaic Solar Energy Conversion*, Vienna, Austria, 1998; p 256.
(17) Rothenberger, G.; Comte, P.; Grätzel, M. *Sol. Energy Mater. Sol. Cells* **1999**, *58*, 321.
(18) Usami, A. *Sol. Energy Mater. Sol. Cells* **2000**, *64*, 73.
(19) Vargas, W. E.; Niklasson, G. A. *Sol. Energy Mater. Sol. Cells* **2001**, *69*, 147.
(20) n is the refractive index of the medium into which the scattering centers are embedded. Here, the scattering centers are each constituent particles of the nanocrystalline films. If we model the films as packing particles in the air, it is plausible that n is the refractive index of the air; this is the literal independent scattering model. However, for the dense media, it is well-known that the scattering rate evaluated with this literal independent scattering model is much greater than experimental results.[14,21] Additionally, nanocrystalline films are not the simple dense media of packing particles. In the applications such as the solar cells, the charge transport in the films is essential. Annealing in the film preparation makes the particles interconnected, though particle sizes do not change owing to annealing temperatures much lower than the melting point. Ferrand and Romestain[11] have studied a light scattering loss from the medium: porous Si waveguides. They assumed that the light scattering is attributed to fluctuations of the refractive index of the light-propagating medium. Although the calculated scattering loss does not quantitatively agree with experimental results, these have the same order of magnitude. Here, after their modeling, we assume that the medium surrounding the scattering centers is the nanocrystalline film having an effective refractive index.
(21) Zurk, L. M.; Tsang, L.; Ding, K. H.; Winebrenner, D. P. *J. Opt. Soc. Am. A* **1995**, *12*, 1772.
(22) Usami, A. *Electrochem. Solid-State Lett.* **2003**, *6*, A236.
(23) Boschloo, G.; Fitzmaurice, D. *J. Phys. Chem. B* **1999**, *103*, 2228.
(24) Matsubara, T.; Oishi, T.; Katagiri, A. *J. Electrochem. Soc.* **2002**, *149*, C89.
(25) The Scherrer equation has a dimensionless constant that is determined experimentally. We evaluated the dimensionless constant from an average crystal size in an atomic force microscope image; additionally, the result was checked with a scanning electron microscope image in ref 26.
(26) Hara, K.; Horiguchi, T.; Kinoshita, T.; Sayama, K.; Sugihara, H.; Arakawa, H. *Sol. Energy Mater. Sol. Cells* **2000**, *64*, 115.
(27) This value is reported in refs 23 and 24. We have cross-checked that the value is applicable to the nanocrystalline films in this paper. The film thickness evaluated from the optical interference structure depends on n; the estimated film thickness under $n = 1.6$ agreed with the film thickness evaluated from surface profiler measurements.
(28) We adopt a typical value in ref 29. Reference 24 has reported that the porosity of porous films has a close relation with the effective refractive index of the films. From ref 24, the adopted value of f is expected to be reasonable under the n value. An estimation of f is also presented in the Appendix.
(29) van de Lagemaat, J.; Benkstein, K. D.; Frank, A. J. *J. Phys. Chem. B* **2001**, *105*, 2433.
(30) Kiyono, M *Titanium Dioxide*; Gihoudo: Tokyo, 1991.